Supporting Information For

Discovery of two *ent*-atisane diterpenoid lactones with AChE inhibitory activity from the roots of *Euphorbia fischeriana*

Jiangchun Wei[a,b,c†], Zhiyue Li[a,b†], Min Shan[d], Fengzhi Wu[e], Limin Li[a], Yucui Ma[a], Junhong Wu[a], Xinping Li[a], Yaqian Liu[a], Zhengxi Hu[c*], Yonghui Zhang[c*] and Zhengzhi Wu[a,b*]

Euphorlactone A (**1**), a rare rearranged *ent*-atisane norditerpenoid with an undescribed 3-*nor*-2,4-olide-*ent*-atisane scaffold, together with euphorlactone B (**2**), a new *ent*-atisane diterpenoid with an unprecedented seven-membered lactone ring C, were isolated from the roots of *Euphorbia fischeriana*. Their planar structures incorporating absolute configurations were extensively elucidated by analysis of the 1D and 2D NMR data, electronic circular dichroism (ECD) calculations, $Rh_2(OCOCF_3)_4$-induced ECD curve, and single-crystal X-ray diffraction. Euphorlactone A (ELA) showed a remarkable AChE (acetylcholinesterase) inhibitory activity (IC_{50} = 2.13 ± 0.06 μM, K_i = 0.058 μM), which was five times stronger than the positive control (rivastigmine, IC_{50} = 12.46 ± 0.82 μM), and further *in vitro* enzyme inhibition kinetic analysis and molecular docking studies were performed to investigate the AChE inhibitory mechanism.

S1. General Experimental Procedures

UV spectra were recorded on a JASCO V-650 UV spectrophotometer. MP was determined by A BUCHI B-540 melting point apparatus. Optical rotations were measured with on a JASCO P2000 automatic polarimeter. ^{1}D- and ^{2}D-NMR spectra were recorded on a Bruker Avance 600/400 spectrometer with solvent peaks as references. HRESIMS data were obtained with an Agilent 1290 Infinity liquid chromatography system and an Agilent 6540 UHD Accurate-Mass Q-TOF mass spectrometer. High-performance liquid chromatography (HPLC) data were recorded on an Agilent 1260 instrument equipped with a photo-diode array (PDA) and a YMC C_{18} column (250 × 4.6 mm, 5 μm). Preparative HPLC was a performed on Sanotac instrument China with a UV detector and a YMC C_{18} column (250 × 20 mm, 5 μm). Column chromatographic separations were carried out with silica gel (200-300 mesh, Qingdao Marine Chemical Group Corporation, Qingdao, China), MCI gel CHP20P (75-150 um, Mitsubishi Chemical Co., Japan) and ODS (50 μm, YMC, Kyoto, Japan). TLC was conducted with glass precoated with silica gel GF254 (Yantai Chemical Industrial Institute, Yantai, China). Chromatographic grade methanol and acetonitrile were purchased from Fisher. All other solvents were of chemical grade (Da Mao Chemical Co. Ltd, Tianjin, China).

S2. X-ray crystallographic analysis of **1**

Colorless columnar crystals of **1** were grown by slow evaporation in MeOH/DCM (1:1, *v/v*) solution. Crystal data were obtained on an Xcalibur Eos Gemini diffractometer with graphite-monochromated Cu-Kα radiation (λ = 1.54184Å).

Crystal data of **1**: $C_{19}H_{26}O_3$ (*M* =302.40 g/mol): orthorhombic, space group $P2_12_12_1$ (no. 19), a = 6.22994(11) Å, b = 10.47670(16) Å, c = 24.3448(4) Å, V = 1588.96(4) Å^3, Z = 4, T = 150.00(10) K, μ(Cu Kα) = 0.664 mm^{-1}, *Dcalc* = 1.264 g/cm^3, 6671 reflections measured (7.262° ≤ 2Θ ≤ 147.604°), 2997 unique (R_{int} = 0.0163, R_{sigma} = 0.0188) which were used in all calculations. The final R_1 was 0.0281 (I > 2σ(I)) and wR_2 was 0.0744 (all data), Flack parameter = 0.04(7).

The X-ray crystallographic data of compounds **1** have been deposited at the Cambridge Crystallographic Data Center with deposition numbers CCDC 2096385, which can be obtained free of charge from the www.ccdc.cam.ac.uk.

Table S2-1 Crystal data and structure refinement for **1**.

Identification code	**1**
Empirical formula	$C_{19}H_{26}O_3$
Formula weight	302.40
Temperature/K	150.00(10)
Crystal system	orthorhombic
Space group	$P2_12_12_1$
a/Å	6.22994(11)
b/Å	10.47670(16)
c/Å	24.3448(4)
α/°	90
β/°	90
γ/°	90

Volume/Å^3	1588.96(4)
Z	4
ρ_{calc}g/cm^3	1.264
μ/mm^{-1}	0.664
F(000)	656.0
Crystal size/mm^3	0.14 × 0.11 × 0.09
Radiation	Cu Kα (λ = 1.54184)
2Θ range for data collection/°	7.262 to 147.604
Index ranges	-4 ≤ h ≤ 7, -12 ≤ k ≤ 12, -29 ≤ l ≤ 29
Reflections collected	6671
Independent reflections	2997 [R_{int} = 0.0163, R_{sigma} = 0.0188]
Data/restraints/parameters	2997/0/210
Goodness-of-fit on F^2	1.089
Final R indexes [I>=2σ (I)]	R_1 = 0.0281, wR_2 = 0.0739
Final R indexes [all data]	R_1 = 0.0285, wR_2 = 0.0744
Largest diff. peak/hole / e Å^{-3}	0.11/-0.19
Flack/Hooft parameter	0.04(7)/0.07(6)

Table S2-2 Fractional Atomic Coordinates (×104) and Equivalent Isotropic Displacement Parameters (Å2×103) for 1. Ueq is defined as 1/3 of of the trace of the orthogonalised UIJ tensor.

Atom	***x***	***y***	***z***	**U(eq)**
O1	9488(2)	2579.9(11)	7872.4(5)	37.7(3)
O2	1549.3(18)	3996.3(12)	5637.4(5)	32.6(3)
O3	8576(3)	1389.0(11)	7176.0(5)	40.3(3)
C1	8197(3)	3715.1(14)	7090.9(6)	24.6(3)
C2	8782(3)	2537.3(16)	7410.2(6)	27.7(3)
C4	7714(3)	1133.1(16)	6618.6(6)	29.0(4)
C5	7287(2)	2372.0(14)	6293.1(6)	22.4(3)
C6	5850(3)	2154.5(14)	5788.9(6)	24.8(3)
C7	5886(3)	3327.8(13)	5418.7(6)	23.2(3)
C8	5303(2)	4561.8(14)	5716.9(6)	20.3(3)
C9	6558(2)	4712.1(13)	6264.7(6)	20.2(3)
C10	6503(2)	3513.9(14)	6641.9(6)	21.3(3)
C11	5956(3)	5989.9(14)	6553.6(6)	24.4(3)
C12	4374(2)	6754.7(14)	6198.2(6)	23.5(3)
C13	2346(2)	5941.3(15)	6119.7(6)	24.5(3)
C14	2903(2)	4724.6(15)	5811.9(6)	22.8(3)
C15	5918(3)	5728.2(14)	5356.7(6)	24.4(3)
C16	5360(3)	6972.3(15)	5638.9(6)	24.5(3)
C17	5646(3)	8104.2(16)	5412.9(7)	34.9(4)
C18	9468(3)	361.9(16)	6338.8(8)	38.7(4)
C19	5766(3)	289.0(16)	6722.3(7)	36.7(4)
C20	4299(3)	3296.5(15)	6910.5(6)	25.3(3)

Table S2-3 Anisotropic Displacement Parameters ($Å^2×10^3$) for **1**. The Anisotropic displacement factor exponent takes the form: $-2\pi^2[h^2a^{*2}U_{11}+2hka^*b^*U_{12}+\ldots]$.

Atom	U_{11}	U_{22}	U_{33}	U_{23}	U_{13}	U_{12}
O1	49.5(8)	37.4(6)	26.1(6)	4.9(5)	-12.1(5)	-2.3(6)
O2	22.7(5)	37.0(6)	37.9(6)	-9.3(5)	-1.5(5)	-6.6(5)
O3	64.9(9)	27.1(6)	28.9(6)	2.6(5)	-17.1(6)	0.2(6)
C1	25.7(7)	26.0(7)	22.1(7)	-0.4(6)	-3.4(6)	-3.2(6)
C2	28.6(8)	29.7(7)	24.6(7)	2.1(6)	-1.8(6)	-4.2(7)
C4	39.3(9)	25.0(7)	22.8(7)	0.3(6)	-2.6(6)	-3.2(7)
C5	24.8(7)	22.5(7)	20.0(6)	-0.6(5)	1.4(6)	-2.9(6)
C6	28.7(8)	24.4(7)	21.3(7)	-3.8(5)	1.1(6)	-3.8(6)
C7	24.6(7)	27.5(7)	17.4(6)	-2.5(6)	0.5(6)	-1.9(6)
C8	20.4(7)	23.7(7)	16.8(6)	-0.3(5)	0.4(5)	-2.8(5)
C9	18.8(6)	23.2(7)	18.6(6)	-0.9(5)	-0.3(6)	-3.8(6)
C10	22.1(7)	23.5(7)	18.2(6)	-0.2(5)	-0.7(6)	-3.1(6)
C11	27.8(8)	25.3(7)	20.1(6)	-2.5(6)	-1.7(6)	-4.5(6)
C12	25.1(7)	23.0(7)	22.3(6)	-1.7(5)	1.4(6)	-2.6(6)
C13	20.7(7)	27.9(7)	24.8(7)	0.6(6)	1.4(6)	-1.6(6)
C14	22.1(7)	27.1(7)	19.1(6)	0.2(6)	0.2(6)	-3.0(6)
C15	24.8(7)	28.7(7)	19.7(6)	1.7(6)	1.9(6)	-2.5(6)
C16	23.3(7)	27.9(7)	22.4(6)	0.5(6)	-2.4(6)	-4.0(6)
C17	45.9(10)	30.5(8)	28.3(8)	1.8(7)	1.3(8)	-8.2(8)
C18	43.9(10)	29.7(8)	42.4(9)	2.5(7)	0.2(8)	7.4(8)
C19	53.5(11)	27.7(8)	28.9(8)	1.5(6)	4.0(8)	-11.1(8)
C20	25.1(8)	29.5(7)	21.3(6)	0.5(6)	2.6(6)	-5.0(6)

Table S2-4 Bond Lengths **1.**

Atom	Atom	Length/Å	Atom	Atom	Length/Å
O1	C2	1.209(2)	C8	C9	1.5538(18)
O2	C14	1.214(2)	C8	C14	1.523(2)
O3	C2	1.3374(19)	C8	C15	1.5519(19)
O3	C4	1.4839(19)	C9	C10	1.5558(19)
C1	C2	1.503(2)	C9	C11	1.558(2)
C1	C10	1.534(2)	C10	C20	1.538(2)
C4	C5	1.544(2)	C11	C12	1.537(2)
C4	C18	1.520(3)	C12	C13	1.536(2)
C4	C19	1.523(2)	C12	C16	1.511(2)
C5	C6	1.536(2)	C13	C14	1.519(2)
C5	C10	1.5461(19)	C15	C16	1.514(2)
C6	C7	1.524(2)	C16	C17	1.319(2)
C7	C8	1.5265(19)			

Table S2-5 Bond Angles for **1.**

Atom	Atom	Atom	Angle/˚	Atom	Atom	Atom	Angle/˚
C2	O3	C4	125.95(12)	C8	C9	C10	114.45(11)
C2	C1	C10	114.99(12)	C8	C9	C11	110.71(12)
O1	C2	O3	117.70(14)	C10	C9	C11	114.93(11)
O1	C2	C1	122.63(15)	C1	C10	C5	106.30(12)
O3	C2	C1	119.65(13)	C1	C10	C9	107.15(11)
O3	C4	C5	112.33(12)	C1	C10	C20	109.37(12)
O3	C4	C18	104.22(14)	C5	C10	C9	107.05(11)
O3	C4	C19	104.00(13)	C20	C10	C5	113.62(12)
C18	C4	C5	109.93(13)	C20	C10	C9	112.95(12)
C18	C4	C19	109.79(14)	C12	C11	C9	110.36(11)
C19	C4	C5	115.84(15)	C13	C12	C11	107.96(12)
C4	C5	C10	115.03(12)	C16	C12	C11	108.98(12)
C6	C5	C4	112.71(12)	C16	C12	C13	107.82(11)
C6	C5	C10	111.71(12)	C14	C13	C12	109.81(12)
C7	C6	C5	110.15(12)	O2	C14	C8	123.95(14)
C6	C7	C8	113.48(11)	O2	C14	C13	122.78(14)
C7	C8	C9	111.99(12)	C13	C14	C8	113.17(13)
C7	C8	C15	109.85(11)	C16	C15	C8	111.40(12)
C14	C8	C7	113.62(12)	C12	C16	C15	111.86(12)
C14	C8	C9	110.62(11)	C17	C16	C12	124.49(14)
C14	C8	C15	103.89(12)	C17	C16	C15	123.62(14)
C15	C8	C9	106.32(11)				

Table S2-6 Torsion Angles for **1.**

A	B	C	D	Angle/˚	A	B	C	D	Angle/˚
O3	C4	C5	C6	-164.40(13)	C9	C8	C14	O2	-131.74(15)
O3	C4	C5	C10	-34.8(2)	C9	C8	C14	C13	51.80(16)
C2	O3	C4	C5	6.6(2)	C9	C8	C15	C16	-58.74(15)
C2	O3	C4	C18	125.55(18)	C9	C11	C12	C13	60.28(15)
C2	O3	C4	C19	-119.42(18)	C9	C11	C12	C16	-56.58(15)
C2	C1	C10	C5	-51.10(17)	C10	C1	C2	O1	-154.86(16)
C2	C1	C10	C9	-165.31(13)	C10	C1	C2	O3	26.9(2)
C2	C1	C10	C20	71.95(17)	C10	C5	C6	C7	61.05(16)
C4	O3	C2	O1	178.96(17)	C10	C9	C11	C12	-134.16(13)
C4	O3	C2	C1	-2.7(3)	C11	C9	C10	C1	-62.61(16)
C4	C5	C6	C7	-167.63(13)	C11	C9	C10	C5	-176.31(12)
C4	C5	C10	C1	55.89(17)	C11	C9	C10	C20	57.89(16)
C4	C5	C10	C9	170.16(12)	C11	C12	C13	C14	-62.67(14)
C4	C5	C10	C20	-64.44(17)	C11	C12	C16	C15	58.25(16)
C5	C6	C7	C8	-54.14(17)	C11	C12	C16	C17	-123.70(17)
C6	C5	C10	C1	-173.99(12)	C12	C13	C14	O2	-170.48(14)
C6	C5	C10	C9	-59.72(15)	C12	C13	C14	C8	6.02(16)

A	B	C	D	Angle/˚	A	B	C	D	Angle/˚
C6	C5	C10	C20	65.68(15)	C13	C12	C16	C15	-58.70(16)
C6	C7	C8	C9	48.13(16)	C13	C12	C16	C17	119.36(18)
C6	C7	C8	C14	-78.10(16)	C14	C8	C9	C10	78.73(15)
C6	C7	C8	C15	166.03(13)	C14	C8	C9	C11	-53.10(16)
C7	C8	C9	C10	-49.12(16)	C14	C8	C15	C16	58.02(15)
C7	C8	C9	C11	179.06(12)	C15	C8	C9	C10	-169.10(12)
C7	C8	C14	O2	-4.8(2)	C15	C8	C9	C11	59.07(14)
C7	C8	C14	C13	178.75(11)	C15	C8	C14	O2	114.54(16)
C7	C8	C15	C16	179.89(13)	C15	C8	C14	C13	-61.92(14)
C8	C9	C10	C1	167.62(12)	C16	C12	C13	C14	54.94(15)
C8	C9	C10	C5	53.93(16)	C18	C4	C5	C6	80.05(17)
C8	C9	C10	C20	-71.88(15)	C18	C4	C5	C10	-150.32(14)
C8	C9	C11	C12	-2.58(16)	C19	C4	C5	C6	-45.10(18)
C8	C15	C16	C12	0.59(18)	C19	C4	C5	C10	84.54(16)
C8	C15	C16	C17	-177.49(16)					

Table S2-7 Hydrogen Atom Coordinates (Å×10^4) and Isotropic Displacement Parameters (Å^2×10^3) for **1.**

Atom	*x*	*y*	*z*	U(eq)
H1A	9487.28	4052.43	6921.78	30
H1B	7669.13	4353.86	7345.81	30
H5	8684.68	2630.91	6146.09	27
H6A	6357.46	1417.35	5585.7	30
H6B	4390.89	1985.76	5907.1	30
H7A	4884.52	3198.61	5118.62	28
H7B	7308.77	3416.59	5261.66	28
H9	8064.58	4808.97	6156.86	24
H11A	5309.67	5810.87	6907.84	29
H11B	7243.53	6490.59	6614.96	29
H12	4020.24	7569.77	6373.7	28
H13A	1737.93	5729.52	6475.06	29
H13B	1283.86	6421.82	5914.37	29
H15A	7446.22	5706.94	5281.19	29
H15B	5163.62	5678.24	5008.82	29
H17A	6340(40)	8180(20)	5052(9)	43(6)
H17B	5210(40)	8900(20)	5608(9)	46(6)
H18A	10731.14	878.82	6300.2	58
H18B	8983.11	95.58	5982.47	58
H18C	9796.71	-375.77	6557.08	58
H19A	6206.33	-470.57	6911.89	55
H19B	5120.83	61.04	6377.88	55
H19C	4742.46	744.44	6942.5	55
H20A	3770	4089.59	7054.37	38

Atom	*x*	*y*	*z*	U(eq)
H20B	4438.05	2689.23	7203.59	38
H20C	3311.97	2975.04	6641.01	38

S3. Calculation of ECD Spectra for **1**.

In general, conformational analyses were carried out via random searching in the Sybyl-X 2.0 using the MMFF94S force field with an energy cutoff of 2.5 kcal/mol (Sybyl Software, 2013). The results showed two lowest energy conformer for both compounds. Subsequently, the conformers were re-optimized using DFT at the PBE0-D3(BJ)/def2-SVP level in MeOH using the polarizable conductor calculation model (SMD) by the ORCA4.2.1 program (Stephens and Harada, 2010; Neese, 2012). The energies, oscillator strengths, and rotational strengths (velocity) of the first 100 electronic excitations were calculated using the TDDFT methodology at the DSD-PBEP86/def2-TZVP level in MeOH. The ECD spectra were simulated by the overlapping Gaussian function (half the bandwidth at 1/e peak height, sigma = 0.30 for all) (Neese, 2017). To get the final spectra, the simulated spectra of the conformers were averaged according to the Boltzmann distribution theory and their relative Gibbs free energy (ΔG). By comparing the experiment spectra with the calculated model molecules, the absolute configuration of the only chiral center was determined to be.

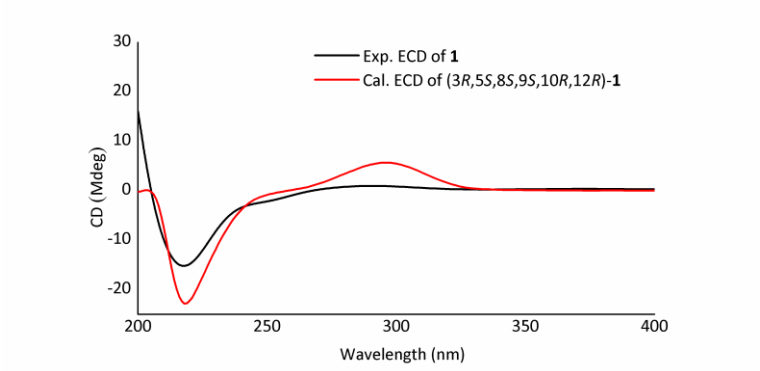

Figure S3. Experimental and calculated ECD spectra of **1** in MeOH.

Table S3. Energy Analysis for the Conformers of **1**.

Conformers	ΔG	P(%)/100	Single point energy(a.u.)
1-1_tddft_	0.00000	52.27	-1041.8189217343
1-2_tddft_	0.00009	47.73	-1041.8188361719

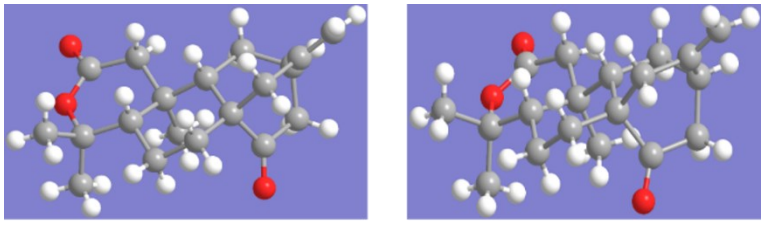

1-1 1-2

Figure S3. B3lyp/6-311g**/20 optimized low-energy conformers of **1**.

S4. Calculation of ECD Spectra for **2.**

In general, conformational analyses were carried out via random searching in the Sybyl-X 2.0 using the MMFF94S force field with an energy cutoff of 2.5 kcal/mol (Sybyl Software, 2013). The results showed six lowest energy conformer for both compounds. Subsequently, the conformers were re-optimized using DFT at the PBE0-D3(BJ)/def2-SVP level in MeOH using the polarizable conductor calculation model (SMD) by the ORCA4.2.1 program (Stephens and Harada, 2010; Neese, 2012). The energies, oscillator strengths, and rotational strengths (velocity) of the first 30 electronic excitations were calculated using the TDDFT methodology at the PBE0-D3(BJ)/def2-TZVP level in MeOH. The ECD spectra were simulated by the overlapping Gaussian function (half the bandwidth at 1/e peak height, sigma = 0.30 for all) (Neese, 2017). To get the final spectra, the simulated spectra of the conformers were averaged according to the Boltzmann distribution theory and their relative Gibbs free energy (ΔG). By comparing the experiment spectra with the calculated model molecules, the absolute configuration of the only chiral center was determined to be.

Table S4. Energy Analysis for the Conformers of **2**.

Conformers	ΔG	P(%)/100	Single point energy(a.u.)
2-1_tddft_	0.00000	42.41	-1005.1598274396
2-2_tddft_	0.00005	40.29	-1005.1597789402
2-3_tddft_	0.00085	17.3	-1005.1589813893
2-4_tddft_	0.01250	0.0	-1005.1473287906
2-5_tddft_	0.01345	0.0	-1005.1463754076
2-6_tddft_	0.01327	0.0	-1005.1465567074

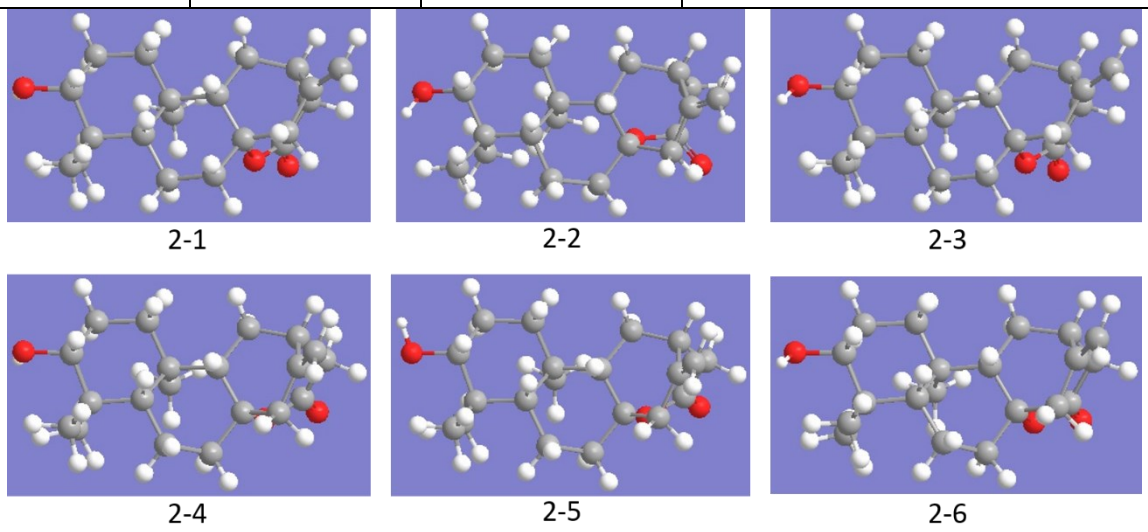

Figure S4. B3lyp/6-311g**/20 optimized low-energy conformers of **2**.

S5. IC_{50} Data of compound **1**

Table S5-1. The residual activity of acetylcholinesterase was incubated with different concentrations of **1** in an *in vitro* activity screening model ($\bar{X} \pm S$, n = 3).

		X	Group A	Group B	Group C	Group D
		concentration	residual activity-A	sidual activity-	sidual activity-	Title
		X	Y	Y	Y	Y
1	Title	0.5	92.49012	93.84010	92.40838	
2	Title	1.0	73.51779	67.62779	72.90576	
3	Title	2.0	41.63373	48.36173	45.68063	
4	Title	4.0	30.83004	32.89646	34.55497	
5	Title	6.0	23.58366	21.23198	24.21466	
6	Title	8.0	16.86430	16.38270	16.75393	
7	Title	10.0	14.75626	14.80996	15.31414	
8	Title					
9	Title					

Table S5-2. Transform X of Table S11-2 ($\bar{X} \pm S$, n = 3).

	X	A	B	C
	concentration	residual activity-A	residual activity-B	residual activity-C
	X			
1	-0.301	92.490	93.840	92.408
2	0.000	73.518	67.628	72.906
3	0.301	41.634	48.362	45.681
4	0.602	30.830	32.896	34.555
5	0.778	23.584	21.232	24.215
6	0.903	16.864	16.383	16.754
7	1.000	14.756	14.810	15.314
8				

Table S5-3. The calculation interface of IC_{50} value of compound **1**.

	Nonlin fit Table of results	A residual activity-A	B residual activity-B	C residual activity-C
1	**log(inhibitor) vs. normalized response -- Variable slope**			
2	**Best-fit values**			
3	LogIC50	0.3153	0.3246	0.3426
4	HillSlope	-1.269	-1.251	-1.239
5	IC50	2.067	2.112	2.201
6	**95% CI (profile likelihood)**			
7	LogIC50	0.2050 to 0.4201	0.2352 to 0.4098	0.2526 to 0.4284
8	HillSlope	-1.694 to -0.9445	-1.571 to -0.9905	-1.559 to -0.9775
9	IC50	1.603 to 2.631	1.719 to 2.569	1.789 to 2.681
10	**Goodness of Fit**			
11	Degrees of Freedom	5	5	5
12	R squared	0.9708	0.9808	0.9802
13	Sum of Squares	157.3	101.7	103.5
14	Sy.x	5.609	4.510	4.550
15				
16	**Number of points**			
17	# of X values	7	7	7
18	# Y values analyzed	7	7	7

S6. Inhibition kinetic data of compound **1**

Table S6-1. Inhibition kinetics of ELA towards AChE ($\bar{X} \pm S$, n = 3).

Table format: XY	X	Group A	Group B	Group C	Group D	Group E	Group F
	concentration of substrate	0μM	0.5μM	1.0μM	2.0μM	4μM	6μM
	X	Y	Y	Y	Y	Y	Y
1	Title	0.1	0.680000	0.634000	0.474000	0.284000	0.209000	0.134000
2	Title	0.2	1.016000	0.944000	0.738000	0.508000	0.382000	0.256000
3	Title	0.4	1.360000	1.242000	1.054000	0.808000	0.645000	0.482000
4	Title	0.6	1.532000	1.394000	1.226000	0.986000	0.819000	0.652000
5	Title	0.8	1.628000	1.472000	1.333200	1.128000	0.965000	0.802000
6	Title	1.0	1.696000	1.522000	1.382000	1.198000	1.043000	0.888000
7	Title	1.2	1.740000	1.556000	1.429200	1.242800	1.091400	0.940000

Table S6-2. The analysis results of inhibition kinetic data K_m and V_{max} of compound **1**.

Nonlin fit	A	B	C	D	E	F
	0μM	0.5μM	1.0μM	2.0μM	4μM	6μM
	Y	Y	Y	Y	Y	Y
1 Michaelis-Menten						
2 Best-fit values						
3 Vmax	2.033	1.802	1.768	1.783	1.756	1.924
4 Km	0.1988	0.1814	0.2724	0.4908	0.6926	1.190
5 Std. Error						
6 Vmax	0.004029	0.008078	0.01640	0.04341	0.06034	0.1522
7 Km	0.001447	0.003117	0.008024	0.02902	0.04977	0.1594
8 95% Confidence Intervals						
9 Vmax	2.023 to 2.043	1.781 to 1.822	1.725 to 1.810	1.672 to 1.895	1.601 to 1.912	1.533 to 2.315
10 Km	0.1951 to 0.2026	0.1734 to 0.1894	0.2517 to 0.2930	0.4162 to 0.5654	0.5646 to 0.8206	0.7797 to 1.599
11 Goodness of Fit						
12 Degrees of Freedom	5	5	5	5	5	5
13 R square	0.9999	0.9996	0.9992	0.9981	0.9980	0.9961
14 Absolute Sum of Squares	5.780e-005	0.0002605	0.0006143	0.001509	0.001390	0.002299
15 Sy.x	0.003400	0.007218	0.01108	0.01737	0.01667	0.02144
16 Constraints						
17 Km	Km > 0.0	Km > 0.0	Km > 0.0	Km > 0.0	Km > 0.0	Km > 0.0
18						
19 Number of points						
20 Analyzed	7	7	7	7	7	7

S7. Spectroscopic data

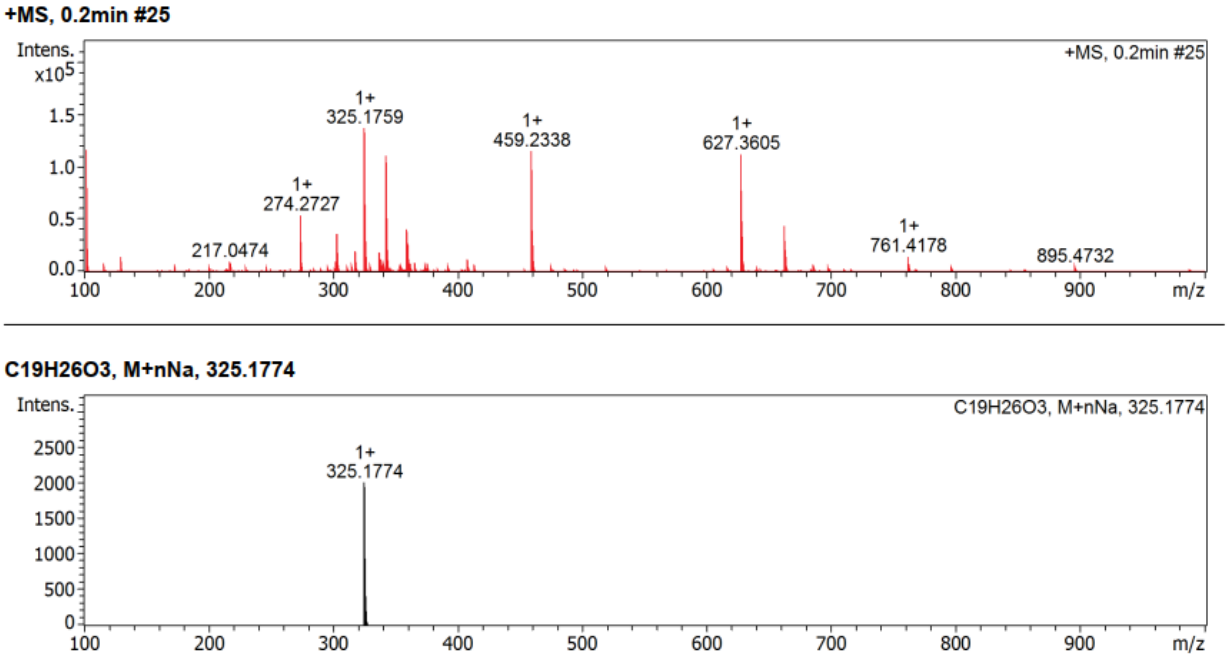

Figure S7-1. The HR-ESIMS Spectrum of compound **1**

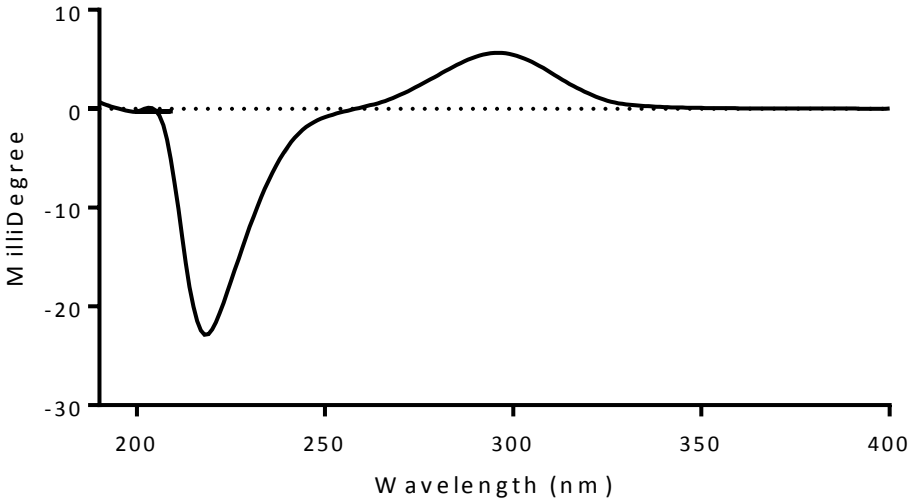

Figure S7-2. CD Spectra of compound **1**

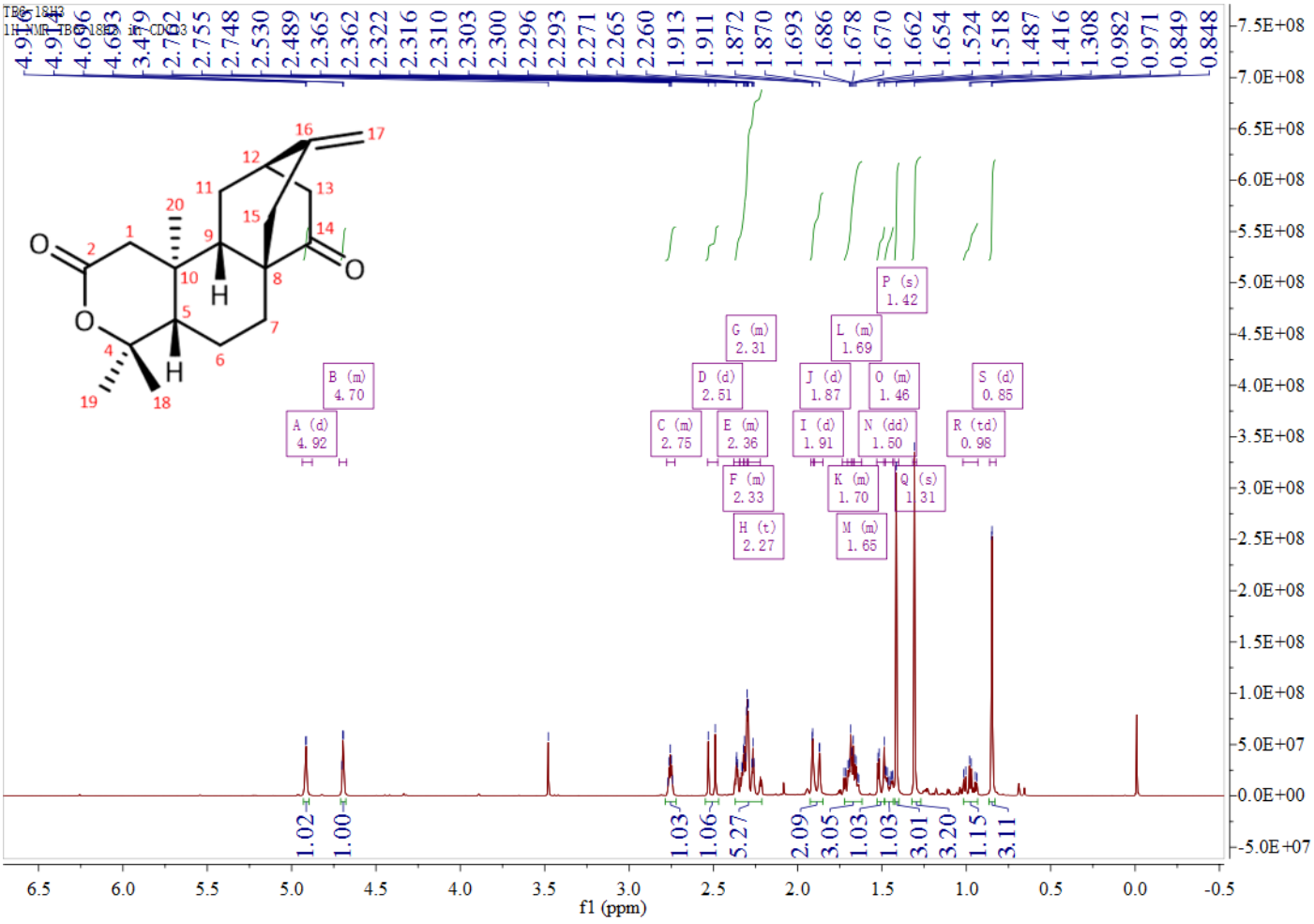

Figure S7-3. The ^{1}H-NMR Spectrum of compound **1** in $CDCl_3$ (400MHz)

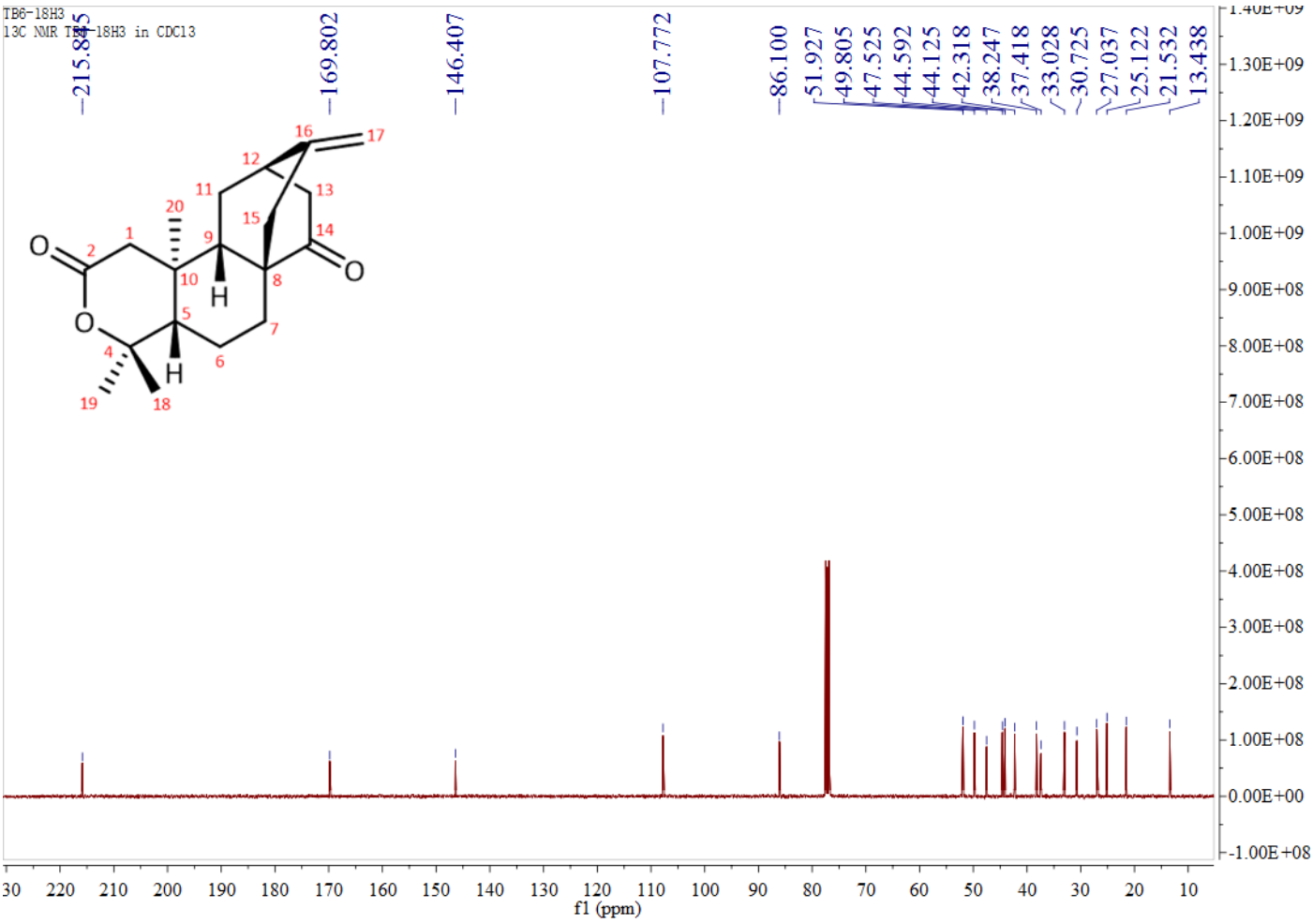

Figure S7-4. The ^{13}C-NMR Spectrum of compound **1** in $CDCl_3$ (100MHz)

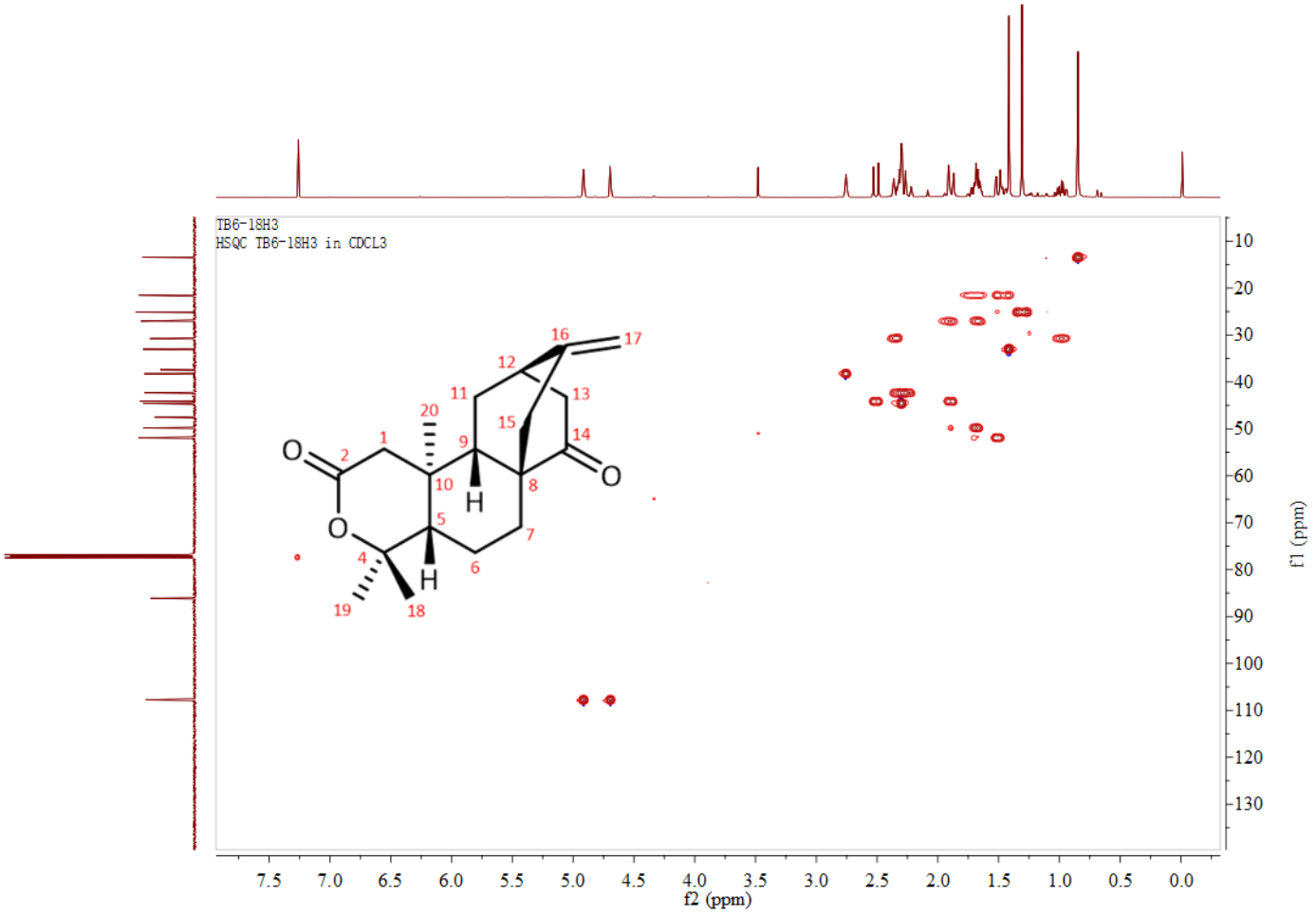

Figure S7-5. The HSQC Spectrum of compound **1** in $CDCl_3$ (400MHz)

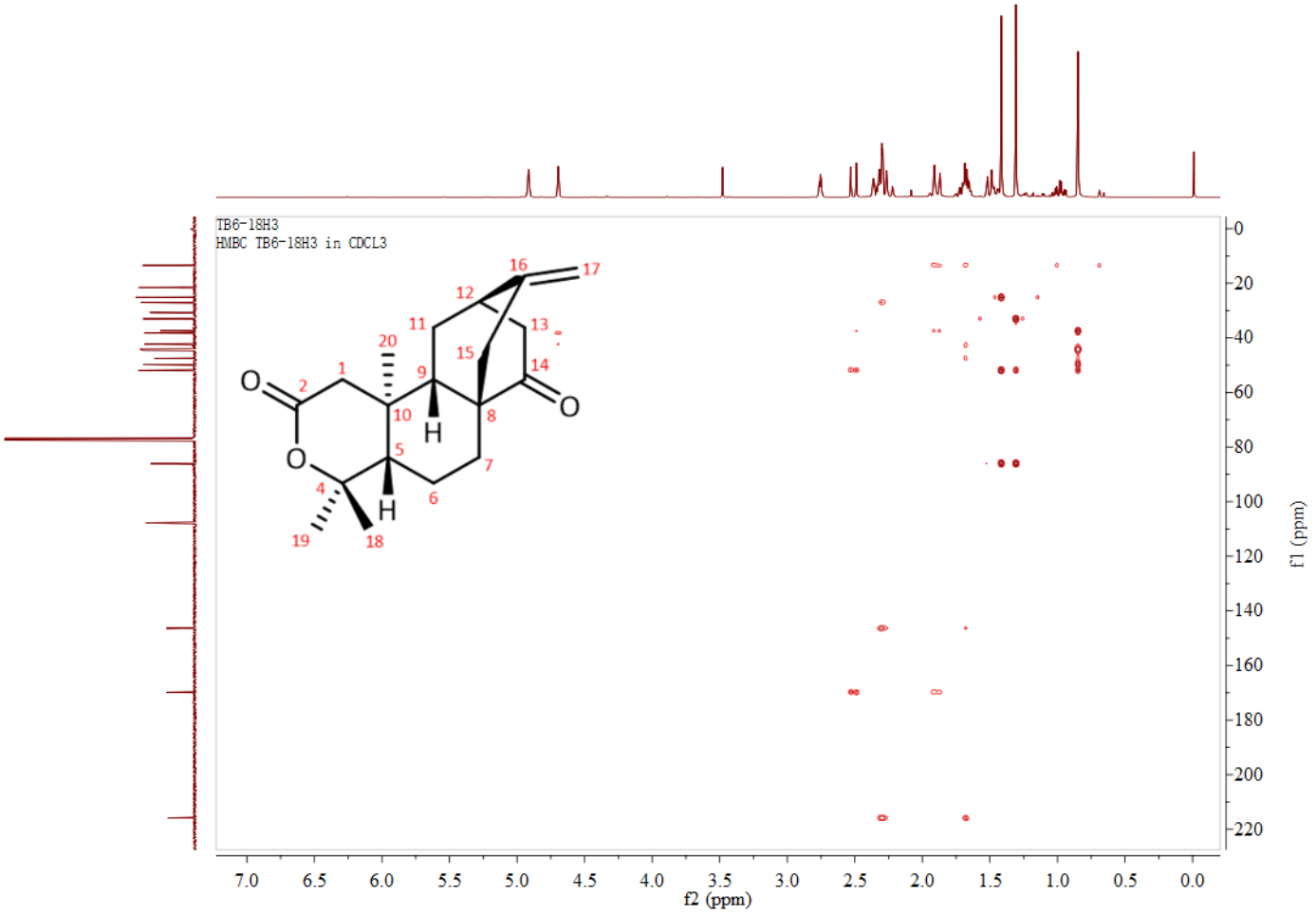

Figure S7-6. The HMBC Spectrum of compound **1** in $CDCl_3$ (400MHz)

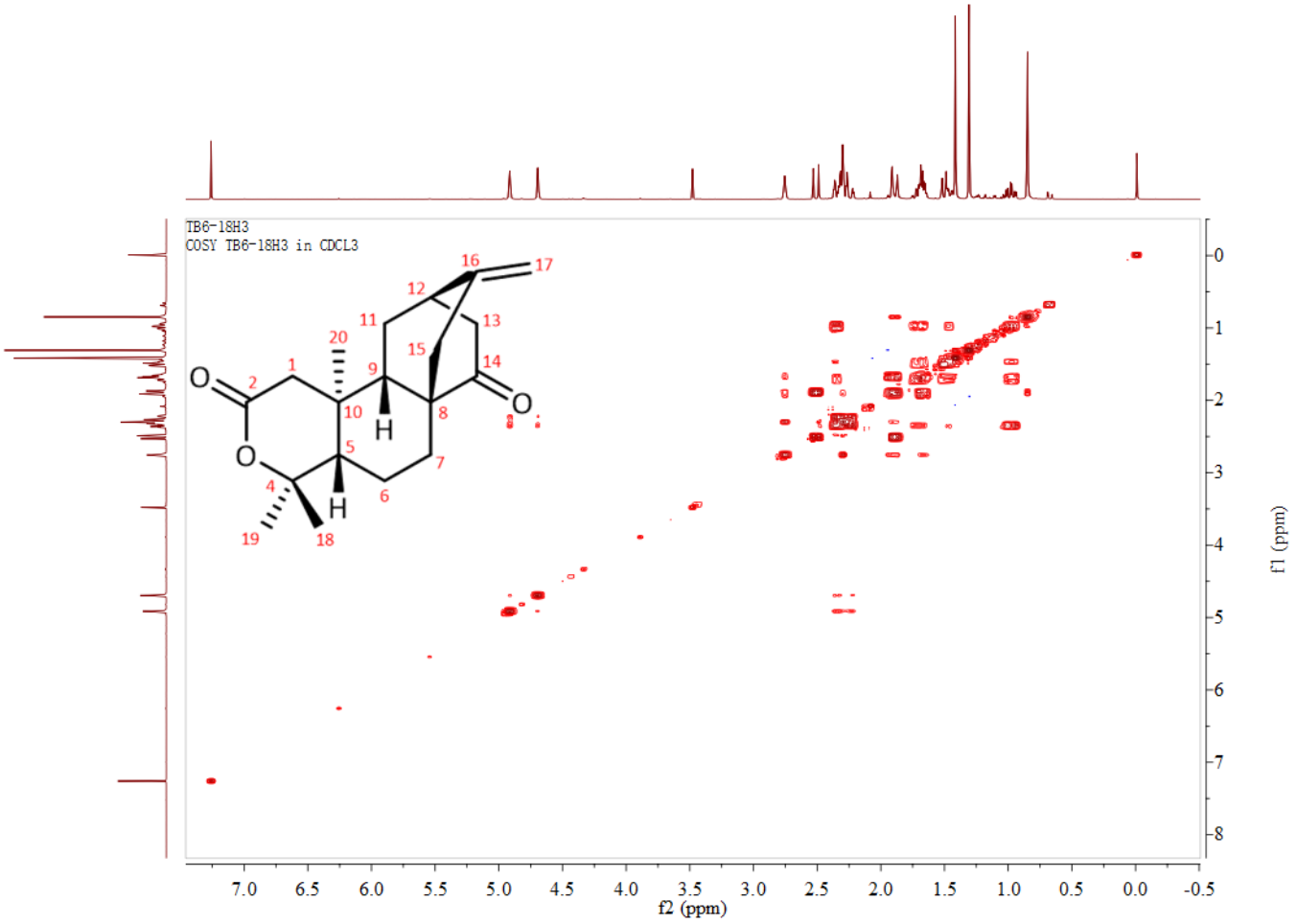

Figure S7-7. The COSY Spectrum of compound **1** in $CDCl_3$ (400MHz)

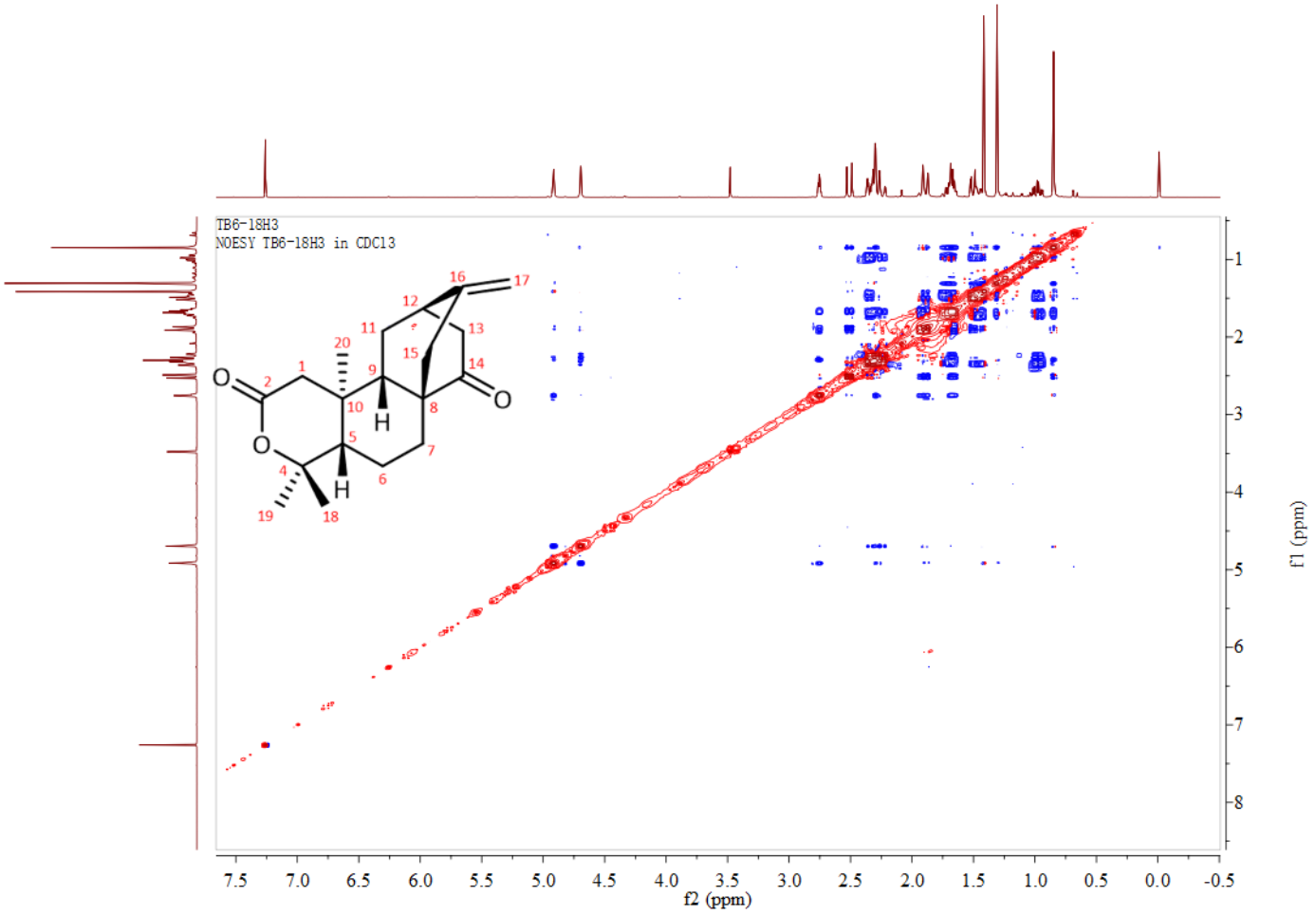

Figure S7-8. The NOESY Spectrum of compound **1** in $CDCl_3$ (400MHz)

Qualitative Analysis Report

Data Filename	SY-TB3.d	**Sample Name**	SY-TB3
Sample Type	Sample	**Position**	P1-B3
Instrument Name	Instrument 1	**User Name**	
Acq Method	s.m	**Acquired Time**	9/8/2020 1:44:51 PM
IRM Calibration Status	Success	**DA Method**	Default.m
Comment			

Sample Group	**Info.**
Acquisition SW Version	6200 series TOF/6500 series Q-TOF B.05.01 (B5125.2)

User Spectra

Fragmentor Voltage	Collision Energy	Ionization Mode
250	0	ESI

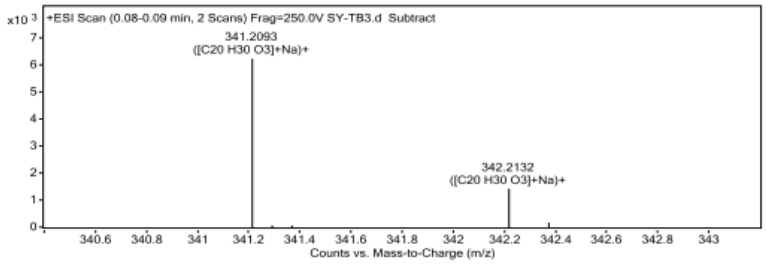

Figure S7-9. The HR-ESIMS Spectrum of compound **2**

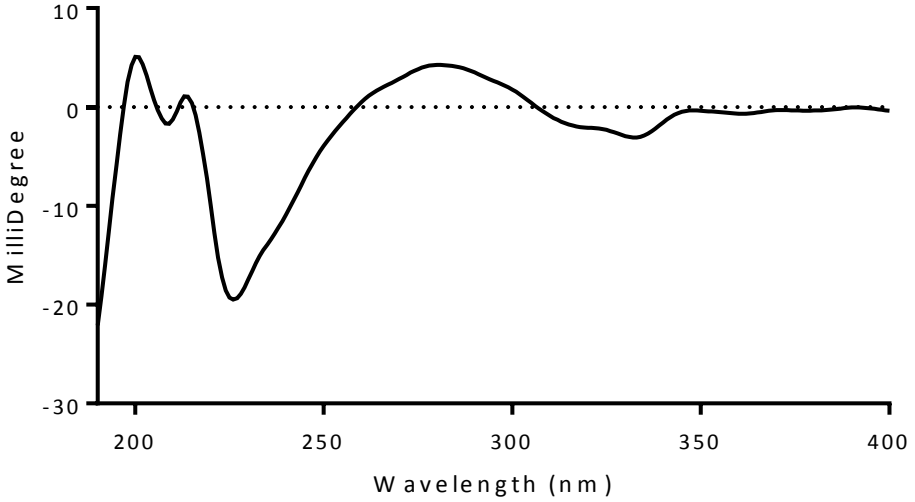

Figure S7-10. CD Spectra of compound **2**

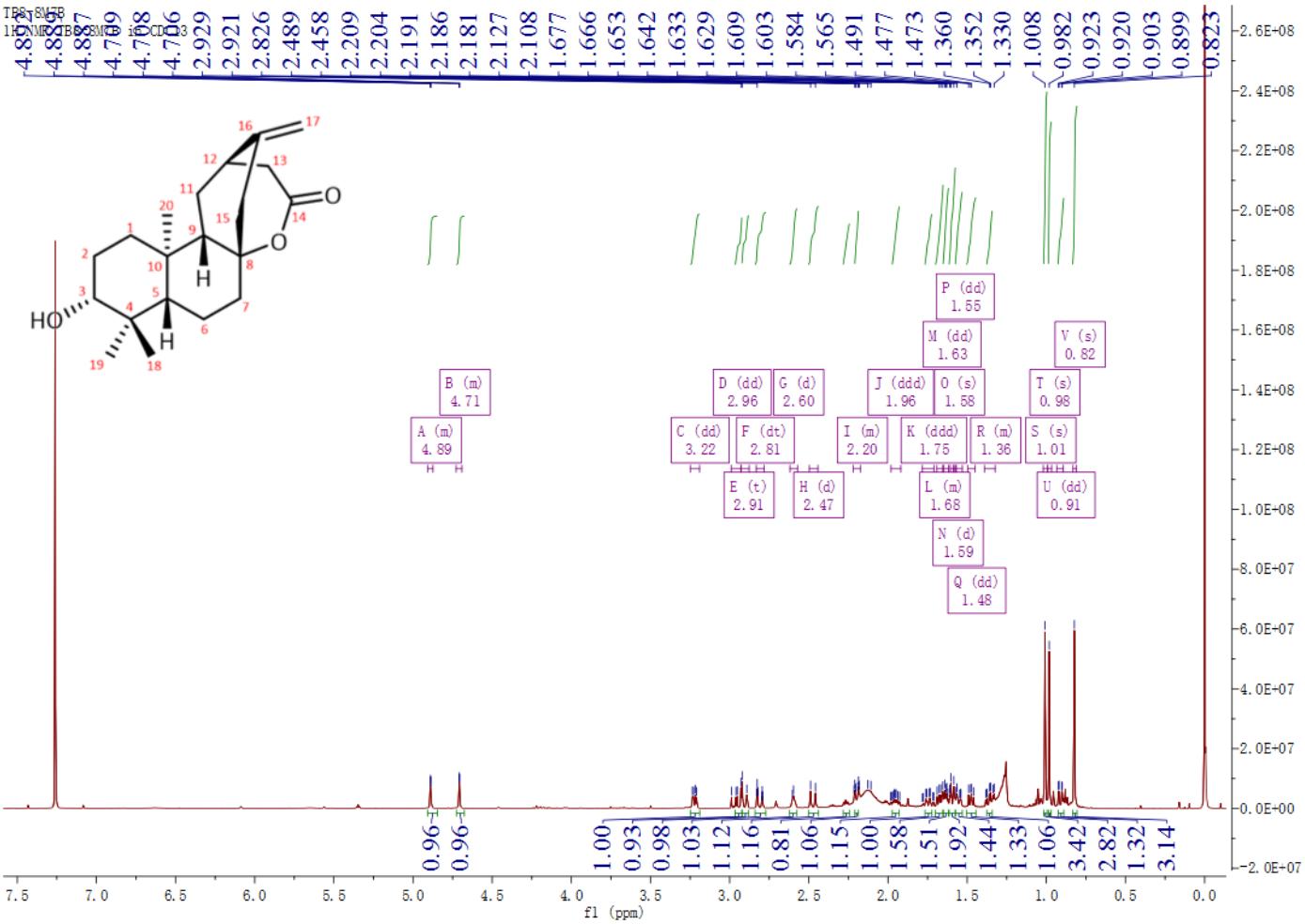

Figure S7-11. The ^{1}H-NMR Spectrum of compound **2** in $CDCl_3$ (600MHz)

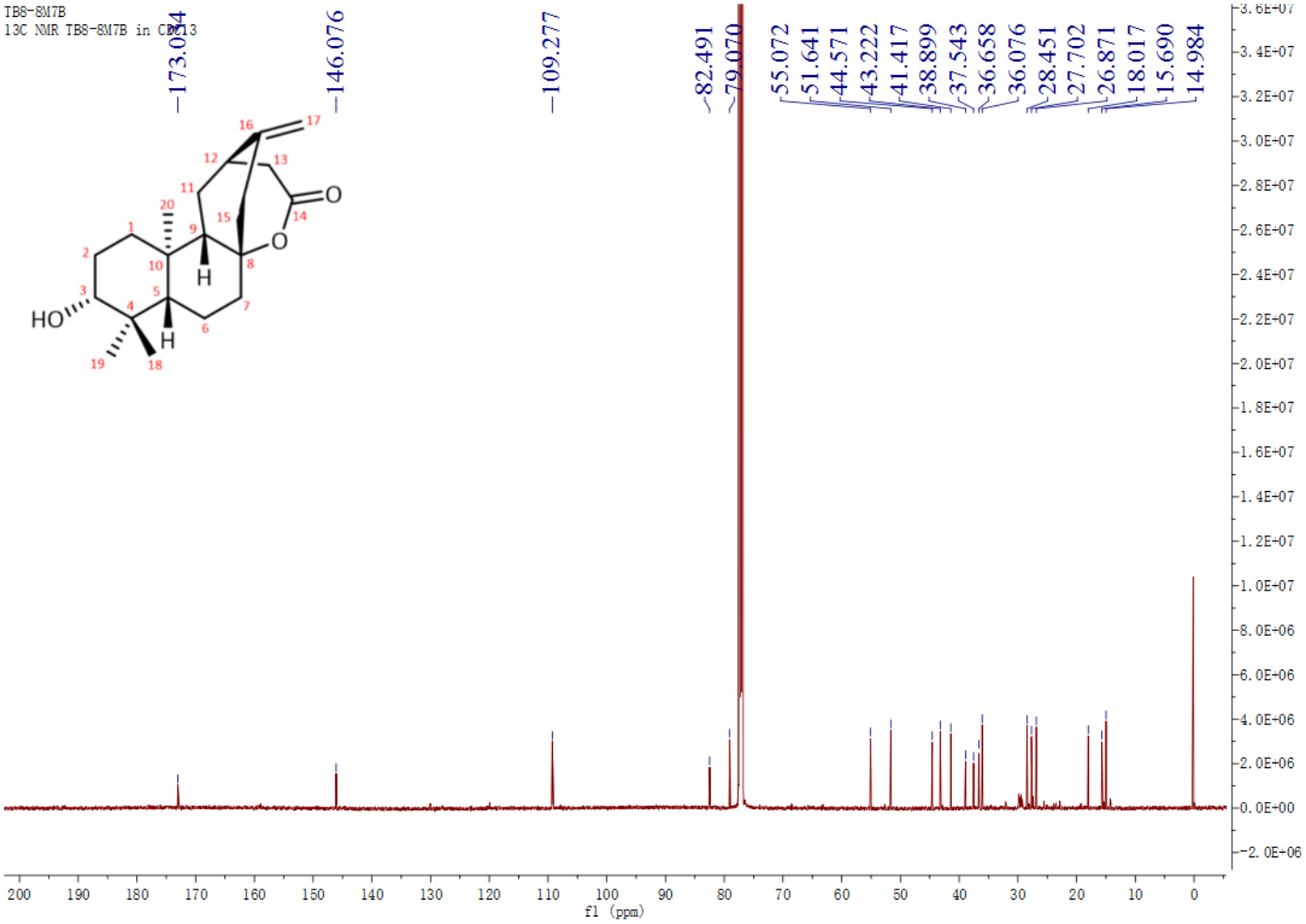

Figure S7-12. The ^{13}C-NMR Spectrum of compound **2** in $CDCl_3$ (150MHz)

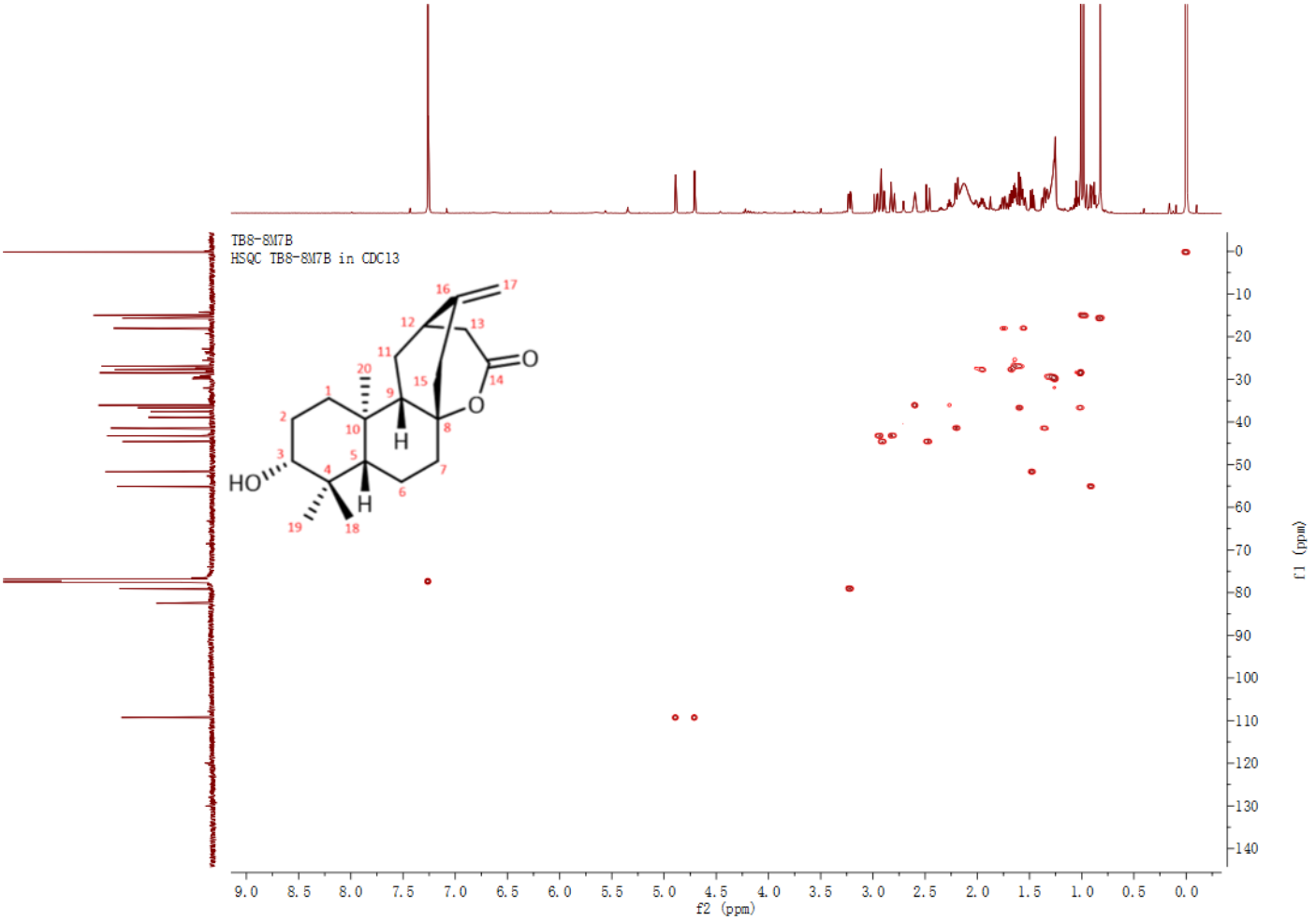

Figure S7-13. The HSQC Spectrum of compound **2** in $CDCl_3$ (600MHz)

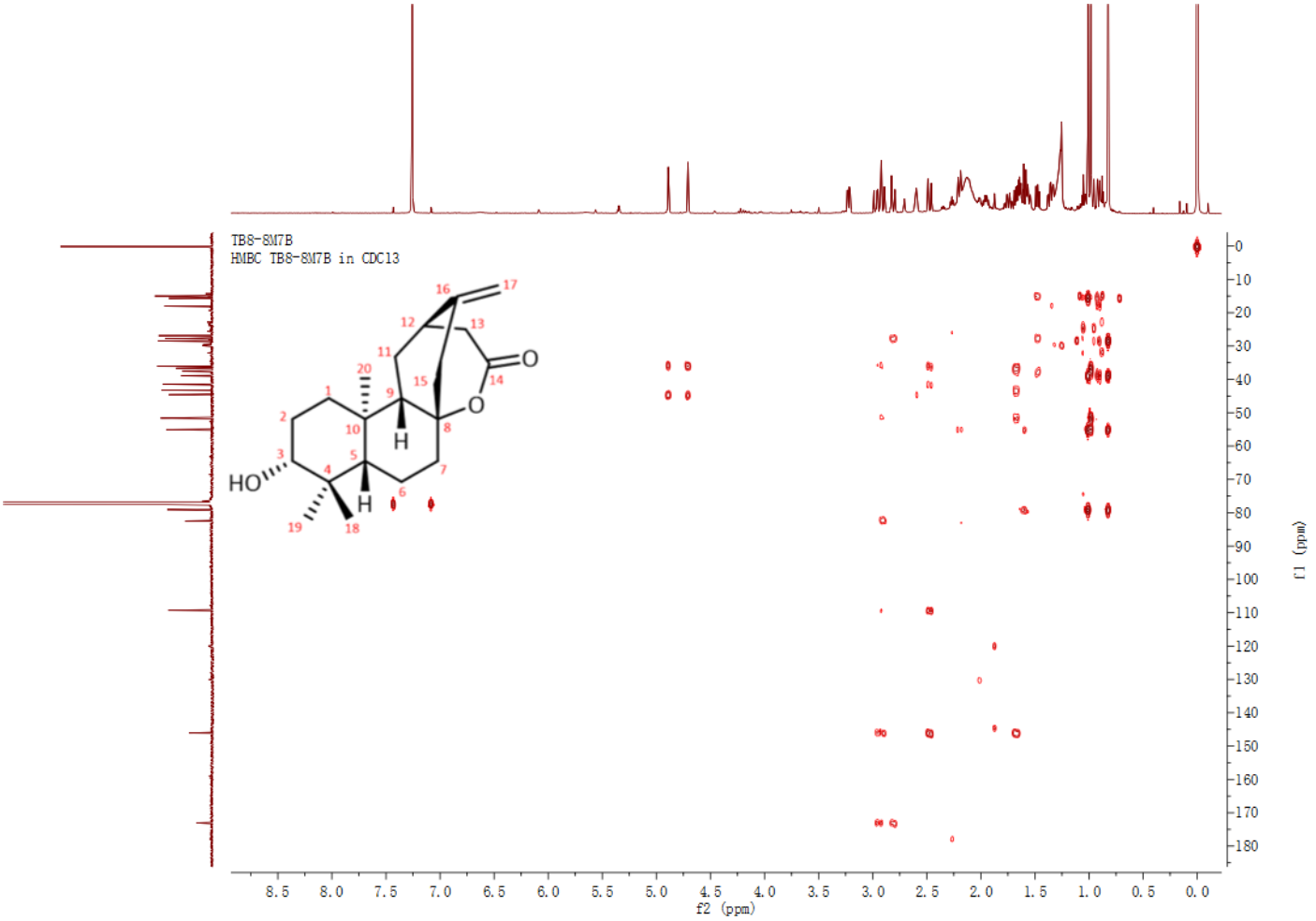

Figure S7-14. The HMBC Spectrum of compound **2** in $CDCl_3$ (600MHz)

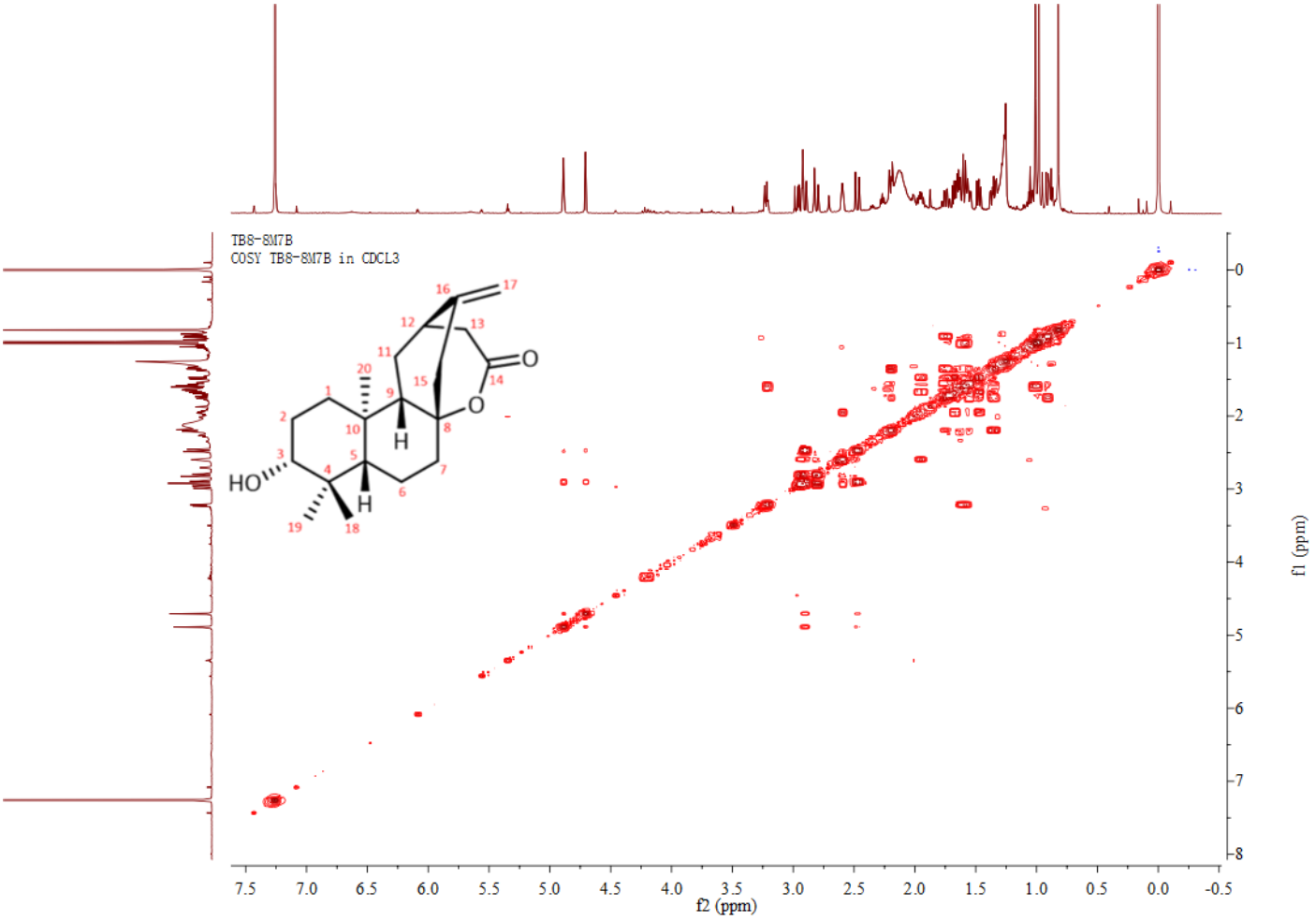

Figure S7-15. The COSY Spectrum of compound **2** in $CDCl_3$ (600MHz)

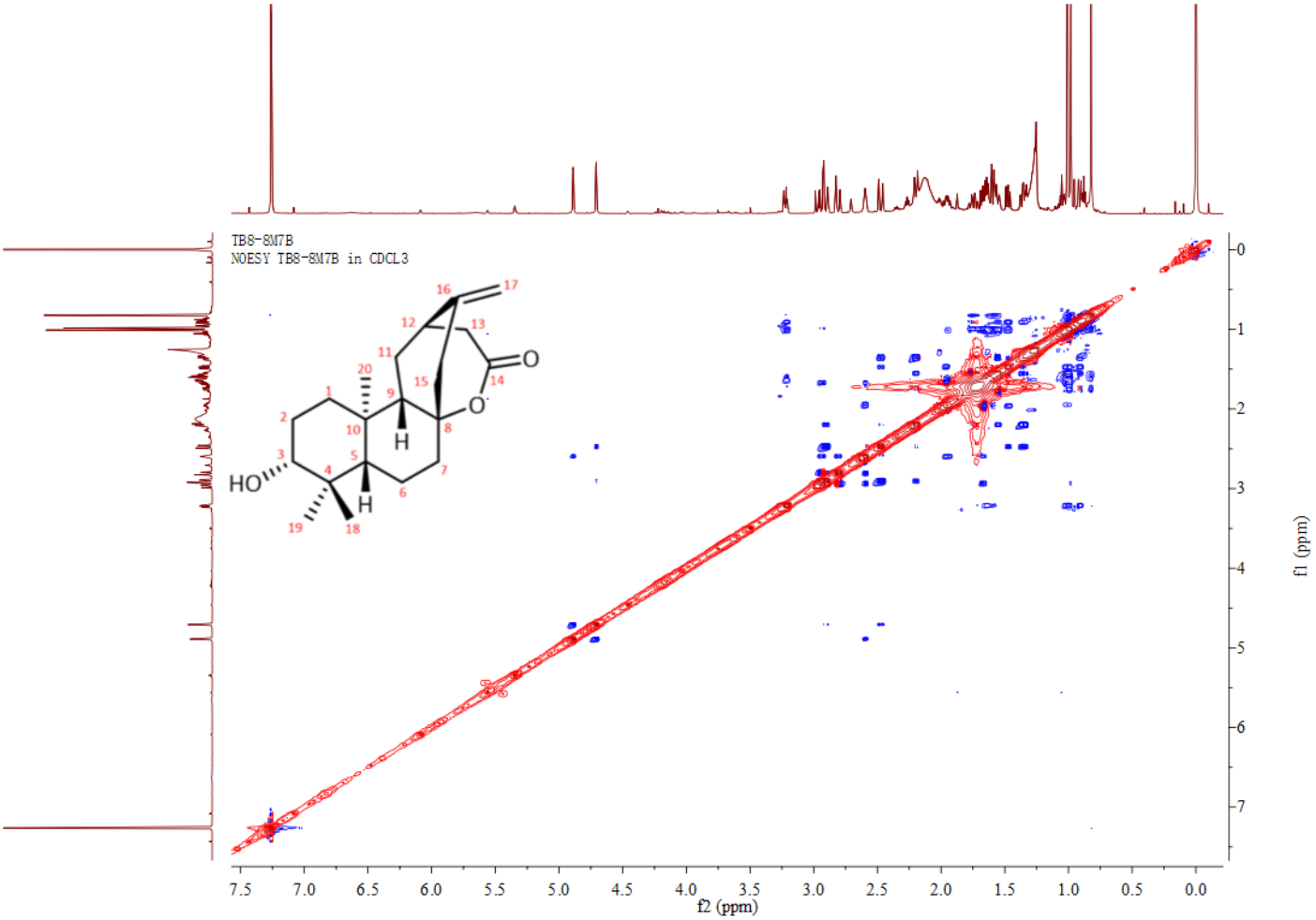

Figure S7-16. The ROESY Spectrum of compound **2** in $CDCl_3$ (600MHz)

S8. References

Neese, F. (2012) Wires. Comput. Mol. Sci. 2, 73-78.

Neese, F. (2017) Wires. Comput. Mol. Sci. 8, e1327.

Stephens, P.J., Harada, N. (2010) Chirality 22, 229–233.

Sybyl Software, version X 2.0; Tripos Associates Inc.: St. Louis, MO, 2013.